

Application of spectromicroscopy tools to explore local origins of sensor activity in quasi-1D oxide nanostructures

A Kolmakov¹, U Lanke², R Karam³, J Shin⁴, S Jesse⁴ and S V Kalinin⁴

¹ Physics Department, SIUC, Carbondale, IL 62901, USA

² Canadian Light Source and Department of Chemistry, University of Saskatchewan, Saskatoon, SK S7N 5C9, Canada

³ Invenios, Inc., 35 South La Patera Lane, Suite C, Santa Barbara, CA 93117-3293, USA

⁴ Condensed Matter Sciences Division, Oak Ridge National Laboratory, Oak Ridge, TN 37831, USA

E-mail: akolmakov@physics.siu.edu

Received 25 May 2006, in final form 23 June 2006

Published 14 July 2006

Online at stacks.iop.org/Nano/17/4014

Abstract

We have tested a range of imaging and spectroscopic techniques to address their ability to locally explore the interplay between surface reactivity and transport properties of the metal oxide nanostructure wired as a chemiresistor and chemi-FET. In particular, we used scanning surface potential microscopy (SSPM) to monitor the spatial and temporal particularities of the dc potential distributions in an operating device. We also successfully implemented synchrotron radiation-based photoelectron emission microscopy (PEEM) to explore submicron lateral compositional and electronic (work function) inhomogeneity on the surface of an individual nanowire sensor. These results open new avenues to visualize and spectroscopically address the chemical phenomena on an individual quasi-1D nanostructure both in real time and at nano- and mesoscopic level.

(Some figures in this article are in colour only in the electronic version)

1. Introduction

The recent tremendous progress in the synthesis, characterization and assembly of quasi-one-dimensional metal oxide nanostructures such as nanowires, nanobelts, nanotubules, etc, when added to their known responsive dependence on the electronic properties from the surface processes make these structures promising active elements to be used in chemical and biological sensors, photovoltaic and nanoelectronic devices and other applications (see [1–3] and references therein). It is generally accepted that appreciable deviation from the macroscopic 3D electronic (and therefore chemical) properties for 1D semiconducting oxides will become prominent when the effective diameter of the nanostructure becomes comparable to the oxide's screening length. For lightly and moderately doped oxides this scale falls into the 10–100 nm range. For such nanostructures the tiny changes in the chemical state of the surface due to the presence of chemical or biological

agents can result in the depletion (or accumulation) of electrons (holes) not only near the surface but in the entire volume of the nanostructure with a concomitant change in its Fermi level position within the bandgap. Combined with the large surface-to-volume ratio, this effective transduction provides the basis for superior chemical sensor function by the oxide nanowire device [4–8]. From the surface chemistry perspective, the same unique features make a nanowire's conducting channel a sensitive 'antenna' of surface catalytic processes [9–11].

Precious structural and compositional as well as dynamic microscopic data on 1D nanostructures were obtained in the past using transmission electron microscopy (TEM), high resolution (HRTEM) and scanning transmission electron microscopy (STEM) (see recent review [12] and references therein). In spite of the apparent superiority in spatial resolution and recent achievements in TEM chemical mapping with electron energy loss spectroscopy (EELS), TEM- and scanning Auger microscopy- (SAM-)based methods are

primarily sensitive to the chemical composition rather than to the chemical state of the surface atoms and routinely induce significant radiation damage in the nano-object.

On the other hand, well-developed synchrotron radiation-(SR)-based photo electron microscopy (PEM) methods such as photoelectron emission microscopy (PEEM) and scanning photoelectron microscopy (SPEM) recently demonstrated steady improvements in spatial resolution passing the threshold of 10 nm [13] and 100 nm respectively [14]. The latter are of particular interest, offering superior sensitivity to the electronic states of the surface atoms and remaining significantly less destructive.

Therefore, it would appear that further exploration of these phenomena will greatly benefit from the experimental technique(s) which are sensitive to the *local* variations of the Fermi level, surface composition and/or electronic structure along the length of 1D nano-object. In electrically contacted nanostructures these properties become inherently coupled with electronic properties of the other parts of the nanodevice (i.e., electrodes, gate oxide, etc). On the other hand, strong variations of the measured parameters from one nanostructure to another are common (due to different diameter (size effects), facet orientation, stoichiometry, doping level, etc). Therefore it is crucial for the measurements to be performed on the *individual* well-characterized nanostructure (not on bundles, arrays or films from the nanostructures). The latter imply that the spectroscopic technique is also a microscopic one with lateral resolution at least not less than the diameter of the nanostructure. To explore these phenomena, surface sensitive and adsorbate specific spectromicroscopic techniques must be applied to *individual* 1D nanostructures wired as an active element of the chemi-FET, chemiresistor or other device.

The surface chemistry is not the only factor determining the performance of nanowire sensors. In real world applications, the entire performance of the nanodevice can depend on the electrostatic inhomogeneities and potential barriers induced by electroactive elements inside the nanostructure (i.e. inherent defects), contact effects and dynamic electrostatic processes taking place on support media (i.e. charging effects) [15]. Scanning surface-potential microscopy (SSPM) uses the scanning AFM cantilever to locally probe the spatial distribution of the potential of the operating nanodevice and therefore is an ideal tool to explore the influence of the latter factors on the transport properties of the nanostructures [16].

In this paper, we describe experimental challenges and demonstrate a few approaches to implement SSPM, PEEM and potentially scanning photoelectron microscopy (SPEM) to study the surface (and bulk) electronic properties of the individual quasi-1D nanostructures mounted in nanodevices. Using PEEM in UV and soft x-ray ranges, we demonstrated the ability of electron spectromicroscopy to reveal submicron lateral particularities in composition and in the core level near edge x-ray absorption fine structure (NEXAFS) of the surfaces of the *individual* metal oxide nanostructures wired as a chemiresistor device.

2. Experiment

Pristine quasi-1D, SnO₂, TiO₂ and In₂O₃ nanostructures up to 500 μm long were synthesized using vapour–solid (VS)

and vapour–liquid–solid (VLS) growth protocols close to those described in [17, 18]. Indium catalyst particles were used to grow In₂O₃ 1D nanostructures, and activated carbon was added into the crucible with TiO₂ powder to facilitate the growth of the titania nanostructures (i.e. carbothermal route). Nanowires were collected from the alumina crucible in which they were formed, and placed on either a Si/SiO₂ wafer for SSPM and gas sensing measurements or on to metallized pillars of the special micromachined dielectric support for the PEEM studies. To preserve the nanostructures' surfaces and the electrode's area from contamination, no wet processes (such as those used in resist-based lithography) were used at any stage of the chemiresistor or chemi-FET device fabrication. The PEEM measurements were conducted at the Canadian Photoelectron Research Spectromicroscope (CaPeRS) facility using a photoelectron emission microscope (PEEM Elmitec GmbH) at the Synchrotron Radiation Center (SRC, Stoughton, WI). The commercial SPM system (Veeco MultiMode NS-IIIa, ORNL) was used to conduct spatially resolved SPM-based dc transport measurements. The sample stage was equipped with a custom-built sample holder, which allows *in situ* biasing of the nanowire sample. SSPM measurements were performed using Pt coated tips (NCSC-12 F, Micromasch) with typical lift heights of 200 nm. The current through the nanostructure was imposed laterally across the surface using vapour deposited Au/Ti macroscopic electrodes. The SPM tip was used as a moving Kelvin probe, providing a spatially resolved dc potential distribution image along the nanostructure.

3. Results and discussion

Using a combination of scanning electron beam microscopy (SEM), macroscopic transport measurements and scanning surface potential microscopy of the SnO₂ nanowire wired as a chemi-FET, we were able to create and directly visualize the influence of local electroactive elements, metal contacts and field-induced mobile charges on the gate oxide layer, which are capable of drastically influencing the sensitivity, stability and response time of the single nanowire sensor.

To model the presence of the electroactive elements along the length of the nanostructure, such as differently doped heterojunctions, the single nanowire chemiresistor device was illuminated locally with a focused electron beam (figure 1). The evolution of the $I_{DS}(V_{DS})$ characteristics of this device was measured as a function of dose (figure 1(e)). As can be seen the conductance through the nanostructure drops significantly upon exposure and then saturates at steady state level. As simple carbonization of the spot would increase the conductivity of the nanowire, we can rule out this possibility because our results (see figure 1(e)) show the opposite trend. We believe that formation of a heterojunction-like area is a more plausible explanation. Due to electron beam induced desorption primarily of oxygen from the SnO₂ nanostructure (see as an example [19]), the illuminated spot gains the concentration of oxygen vacancies thus forming the additional donor states. This locally reduced area develops as a n–n⁺–n junction in the middle part of the structure with relatively shallow barriers which are responsible for a moderate conductance drop. This picture is supported by scanning

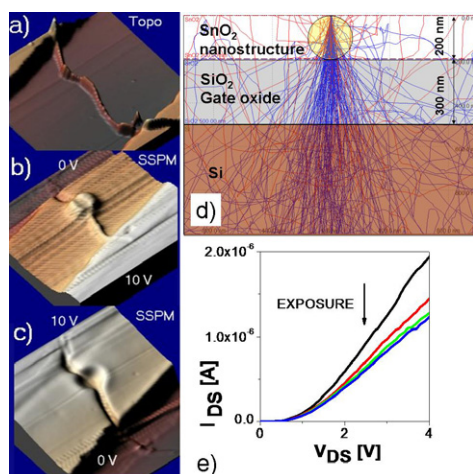


Figure 1. The comparison of topographic $40 \times 40 \mu\text{m}^2$ (a) and SSPM ((b), (c)—taken at opposite polarity) images of single SnO_2 nanowire FET with e-beam fabricated local electroactive defect (Z-scales: 2000 nm for (a) and 10 V for (b), (c)). (d) The simulation of the spatial distribution of the electron beam-induced defects formation in SnO_2 nanowire based FET. The parameters used: SnO_2 NW diameter 200 nm, electron energy 20 kV, normal incidence. (e) Temporal evolution of I_{DS} (V_{DS}) of the SnO_2 nanowire chemiresistor under electron exposure (20 kV, 20 mA, rastering $2.4 \times 10^3 \mu\text{m}^2$ area). The $I(V)$ curves were taken *in situ* sequentially with about 1 min time interval between the scans.

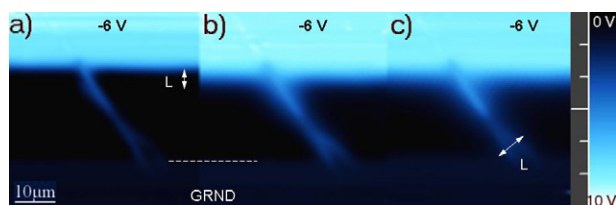


Figure 2. $50 \times 50 \mu\text{m}^2$ SSPM images of the surface potential distribution on and around the biased nanowire (a) 10 min, (b) 18 min and (c) 36 min after application of the negative potential on the top electrode. The smearing of the potential contrast is due to induction and mobility of the surface charges on the gate oxide. L denotes the spatial extension of the charged areas.

potential microscopy data (figures 1(a)–(c)) which is sensitive to the local inhomogeneities of the potential distribution in the biased nanostructure. As shown, the exposure of the middle point of the nanostructure leads to drastic changes in the SSPM map (figures 1(b), (c)); however, no particularities can be seen on the topographic AFM scan (figure 1(a)). However, this simplistic model can be considered only as a preliminary one as more detailed modelling of the interaction volume (figure 1(d)) reveals [20] the formation of a possibly reduced and charged area in the gate oxide. The latter one in turn can induce the additional parasitic gating on the nanostructure which could also cause the reduction of I_{DS} .

The environmental SSPM measurements revealed the importance of the neighbouring gate oxide layer (and generally speaking any support) for the electron transport (and therefore sensing performance) of quasi-1D chemiresistors and chemi-FETs. Figures 2(a)–(c) represent a sequential mapping of the surface potential at the biased SnO_2 nanowire chemiresistor and neighbouring gate oxide area at 10, 18 and 36 min after

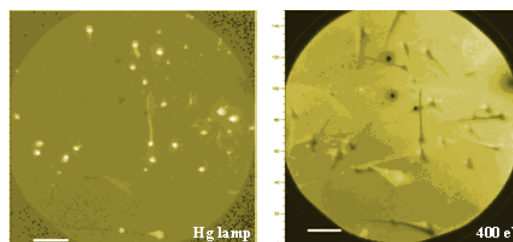


Figure 3. PEEM chemical contrast on In_2O_3 nanowires grown on In catalyst particles: (a) $h\nu = 400 \text{ eV}$; (b) $h\nu = 5 \text{ eV}$. The diameter of the nanostructures is about 300 nm. FOV is $100 \mu\text{m}$.

the bias was applied. The observed gradual spreading of the potential ‘halo’ is due to the induction and mobility of the surface charges present on the oxide surface. Since no resistance was used in our fabrication protocol, the charge accumulation is related to the gate oxide surface. The effect was found to depend strongly on humidity; an effect which can only be eliminated via annealing or UV photodesorption in vacuum. The origin of this effect arises from the high polarizability and mobility of the water molecules and/or hydroxyl species adsorbed on SiO_2 film at ambient conditions [21]. The latter is concomitant with predominant mobilities of the negative charges from the areas of high negative potential such as the top electrode and upper part of the nanostructure (figure 2). As has been illustrated (see as an example [15, 22] and references therein), these surface charge effects manifest themselves in the macroscopic transport measurements as a hysteresis response to the sudden back gate bias and/or in the long term time-dependence of I – V curves. Due to their parasitic electrostatic coupling (gating) with the nanowire conducting channel, these surface charges are able to strongly effect the chemical and biological sensing performance of the FET configured nanowire-based devices operating in real world wet or humid environment. In fact, poorly controlled mobile charges are the primary limitation of ambient dc transport measurements by SSPM. These impediments can in principle be solved by carrying out sensing and transport measurements at high frequency with, for example, scanning impedance microscopy [23]. However, the capacitance coupling with the gate electrode will limit the applicability of this method and therefore the implementation of new supports is required.

Due to its inherent sensitivity to the local variations of the work function, PEEM is an invaluable tool to study morphologically and compositionally inhomogeneous surfaces of the nanostructures. PEEM techniques are especially attractive for exploring the real time surface dynamic process at nano- and meso-scales [24] as well as working electronic microdevices [25]. In figure 3, a few In_2O_3 nanowires are placed on a Si wafer (covered with thin native oxide) and lightly sputtered then imaged in UHV on the same area but at different photon energies. Figure 3(a) shows a photoelectron image with $100 \mu\text{m}$ field of view (FOV) acquired at 400 eV of soft x-rays. The protruding spots represent In nanoparticles used as seeds during the nanostructure growth. The contrast in the image is faint and shows mostly topographic features because at this photon energy the absorption coefficients of Si, In or O do not differ appreciably. In figure 2(b)

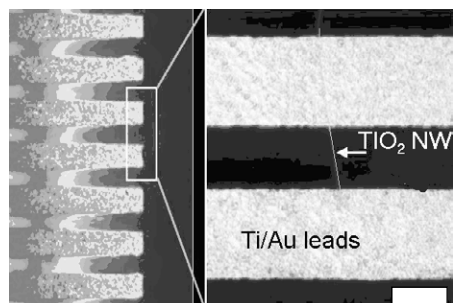


Figure 4. The prospective robust platform for artefact free spectromicroscopy on quasi 1D nanostructures. The width and the distance between the pillars in the support shown is about 65 and 50 μm respectively. The white bar is 50 μm .

on the other hand, the energy of the light was tuned to be just above In work function but a bit below that of the photoemission threshold of In_2O_3 and SiO_2 oxides. A much stronger chemical contrast can be observed in the latter case and In rich nucleation seeds can be clearly seen due to the higher photoemission yield with respect to both In oxide nanowires and Si substrate. These experiments demonstrate the potential of the chemical selectivity of the PEEM imaging of individual 1D nanostructures; such imaging can be used for optimal surface functionalization strategies and spectroscopic visualization of the adsorption/desorption phenomena on individual nanostructured sensing elements both in real time and at nano/mesoscopic level.

However, as shown above, in nanodevice application, electron and synchrotron radiation-based spectromicroscopy face a major experimental challenge due to charging problems similar to those described in [26, 27]. We have tested the prospective design of the support which allowed us to work with complex nanostructures and have not experienced problems with charging even under illumination of the sample with defocused x-ray (UV) photon or electron beams. Taking advantage of the high aspect ratio of 1D nanostructures is the key solution to these experimental impediments, achieved by using the suspended nanostructures where the dielectric areas of the support, which are still able to store the parasitic charge, are spatially and electrically decoupled from the nanostructure. The principle of PEEM on suspended 1D nanostructures is shown in figure 4. Instead of planar Si/ SiO_2 support, the substrate used is nonconducting micromachined glass (Invenios Inc. [28]), which has a dense (about 100 up to 500 cm^{-1}) array of high aspect ratio (~ 10) fine micro-trenches. The metallization of the top and inside of the microwalls was made using two sequential depositions of Ti (100 nm) and Au (1000 nm) while the substrate was tilted at a $\pm 15^\circ$ angle with respect to the metal flux direction. Under these deposition conditions the metallization took place exclusively on top and on the inside of each wall, thus preventing the bottoms of adjacent microwalls from being electrically connected. The latter design drastically cuts charging due to high aspect ratio of the walls since neither primary photons nor secondary electrons penetrate to the interior of the deep nonconducting trenches. Due to high thermal stability of the substrate, the imaging experiments can be conducted up to 600 $^\circ\text{C}$. In addition, this sample design is free from

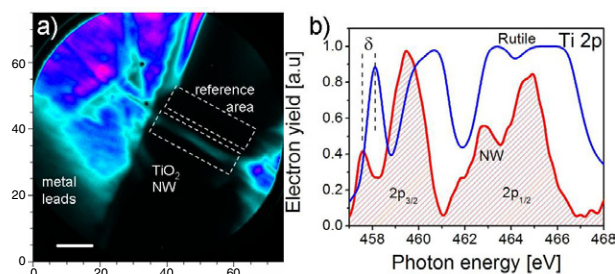


Figure 5. (a) 75 μm FOV PEEM image of the suspended TiO_2 nanowire contacted by two metal electrodes. The image was taken near the O 1s edge (534 eV) due to better contrast with respect to the background. The marked area represents the region where Ti 2p NEXAFS was collected. The reference spectrum was taken from a similar area not containing NW. (b) Comparison of the normalized total electron yield Ti 2p NEXAFS spectra taken from the individual TiO_2 nanowire (filled spectrum) and from the rutile TiO_2 (solid line) crystal. The spectrum from the reference area and featureless background (slope) were subtracted.

the parasitic gating effects (i.e., capacitive coupling with the gate) which are commonly observed during impedance measurements on traditionally FET wired nanostructures. Using this support's design we were able to acquire PEEM images of semiconducting nano- and meso-wires and get spatially resolved NEXAFS spectra from the individual TiO_2 nanowire by varying the excitation energy of the soft x-rays and using the greyscale (electron yield) signal from the nanostructure for spectroscopy (figure 5). As can be seen, not only can spin-orbit splitting of the 2p core states of the individual nanostructure be resolved but also the splitting of the final 3d states due to crystal-field interaction. The detailed analysis of the observed spectral shift and intensity ratios will be published elsewhere.

4. Conclusions

The surface chemistry of metal oxide nanostructures with an effective diameter comparable or smaller than the material's Debye length (10–50 nm) strongly influences their electronic and in particular transport properties. At diameters below 5–7 nm the distinction between ‘surface’ and ‘bulk’ vanishes and the nanostructure's electronic (and chemical) properties can be governed by individual bonding events and quantum confinement effects. The fundamentals of this size-selective surface \leftrightarrow bulk interplay are not only of academic interest but are of key importance for the operation of prospective chemical and bio-sensing, catalysts, optoelectronic and energy conversion devices. In the latter case the progressive reduction of the dimensions of the microdevices induces stronger electronic coupling between an active nanostructure and neighbouring elements of the circuit. To explore these phenomena, surface-sensitive and adsorbate-specific spectromicroscopic techniques have to be implemented for *individual* 1D nanostructures wired as a part of the nanodevice. In this work, using an array of imaging techniques we have demonstrated a few experimental approaches to visualize at the meso- and nanoscale the particularities of the transport phenomena, charge redistribution, work function and chemical composition of the oxide nanostructures relevant to the gas

sensing. We have indicated a few experimental impediments for electron and synchrotron radiation based microscopy on individual nanostructures and proposed their solutions through the use of micromachined supports. Using this methodology for PEEM in UV and soft x-ray ranges, we demonstrated the ability of photo electron spectromicroscopy to reveal submicron lateral particularities in the composition and core level NEXAFS structure of the *individual* metal oxide nanostructures wired as a chemiresistor device. The tested methodology of the ‘charge-free’ supports can be easily scaled down to the 10–100 nm range using modern microfabrication techniques.

Acknowledgments

We thank Dr Y Lilach (PNNL) for his help with the software used for the experiment. The research at SIUC was supported through ORDA's New Faculty Seed Grant. A K thanks the administration of the Synchrotron Radiation Center, University of Wisconsin-Madison, for the travel grant. SRC operation is supported by the NSF under Award No. DMR-0084402. A portion of this research was conducted at the Center for Nanophase Materials Sciences, which is sponsored at Oak Ridge National Laboratory by the Division of Scientific User Facilities, US Department of Energy.

References

- [1] Lieber C M 2003 Nanoscale science and technology: building a big future from small things *MRS Bull.* **28** 486–91
- [2] Xia Y N, Yang P D, Sun Y G, Wu Y Y, Mayers B, Gates B, Yin Y D, Kim F and Yan Y Q 2003 One-dimensional nanostructures: synthesis, characterization, and applications *Adv. Mater.* **15** 353–89
- [3] Wang Z L 2004 Functional oxide nanobelts: materials, properties and potential applications in nanosystems and biotechnology *Annu. Rev. Phys. Chem.* **55** 159–96
- [4] Cui Y, Wei Q Q, Park H K and Lieber C M 2001 Nanowire nanosensors for highly sensitive and selective detection of biological and chemical species *Science* **293** 1289–92
- [5] Law M, Kind H, Messer B, Kim F and Yang P D 2002 Photochemical sensing of NO₂ with SnO₂ nanoribbon nanosensors at room temperature *Angew. Chem. Int. Edn* **41** 2405–8
- [6] Comini E, Faglia G, Sberveglieri G, Pan Z W and Wang Z L 2002 Stable and highly sensitive gas sensors based on semiconducting oxide nanobelts *Appl. Phys. Lett.* **81** 1869–71
- [7] Kolmakov A, Zhang Y, Cheng G and Moskovits M 2003 Detection of CO and oxygen using tin oxide nanowire sensors *Adv. Mater.* **15** 997–1000
- [8] Zhang D H, Liu Z Q, Li C, Tang T, Liu X L, Han S, Lei B and Zhou C W 2004 Detection of NO₂ down to ppb levels using individual and multiple In₂O₃ nanowire devices *Nano Lett.* **4** 1919–24
- [9] Zhang Y, Kolmakov A, Chretien S, Metiu H and Moskovits M 2004 Control of catalytic reactions at the surface of a metal oxide nanowire by manipulating electron density inside it *Nano Lett.* **4** 403–7
- [10] Kolmakov A and Moskovits M 2004 Chemical sensing and catalysis by one-dimensional metal-oxide nanostructures *Annu. Rev. Mater. Res.* **34** 151–80
- [11] Zhang Y, Kolmakov A, Lilach Y and Moskovits M 2005 Electronic control of chemistry and catalysis at the surface of an individual tin oxide nanowire *J. Phys. Chem. B* **109** 1923–9
- [12] Wang Z L 2003 New developments in transmission electron microscopy for nanotechnology *Adv. Mater.* **15** 1497–514
- [13] Frazer B H, Girasole M, Wiese L M, Franz T and De Stasio G 2004 Spectromicroscope for the photoelectron imaging of nanostructures with x-rays (SPHINX): performance in biology, medicine and geology *Ultramicroscopy* **99** 87–94
- [14] Gunther S, Kaulich B, Gregoratti L and Kiskinova M 2002 Photoelectron microscopy and applications in surface and materials science *Prog. Surf. Sci.* **70** 187–260
- [15] Kalinin S V, Shin J, Jesse S, Geohegan D, Baddorf A P, Lilach Y, Moskovits M and Kolmakov A 2005 Electronic transport imaging in a multiwire SnO₂ chemical field-effect transistor device *J. Appl. Phys.* **98** 044503
- [16] Nonnenmacher M, Oboyle M P and Wickramasinghe H K 1991 Kelvin probe force microscopy *Appl. Phys. Lett.* **58** 2921–3
- [17] Dai Z R, Gole J L, Stout J D and Wang Z L 2002 Tin oxide nanowires, nanoribbons, and nanotubes *J. Phys. Chem. B* **106** 1274–9
- [18] Rao C N R, Gundiah G, Deepak F L, Govindaraj A and Cheetham A K 2004 Carbon-assisted synthesis of inorganic nanowires *J. Mater. Chem.* **14** 440–50
- [19] Erickson J V 1989 Electron, ion, and photon beam induced reduction of SnO₂(110): power dissipation thresholds *J. Vac. Sci. Technol. B* **7** 1265–74
- [20] Drouin D, Hovington R, Horny P, Demers H, Couture A R and Gauvin R 2002 CASINO: Monte Carlo simulation of electron trajectory in solids <http://www.gel.usherbrooke.ca/casino/index.html>
- [21] Kim W, Javey A, Vermesh O, Wang O, Li Y M and Dai H J 2003 Hysteresis caused by water molecules in carbon nanotube field-effect transistors *Nano Lett.* **3** 193–8
- [22] Goldberger J, Sirbully D J, Law M and Yang P 2005 ZnO nanowire transistors *J. Phys. Chem. B* **109** 9–14
- [23] Bachtold A, Fuhrer M S, Plyasunov S, Forero M, Anderson E H, Zettl A and McEuen P L 2000 Scanned probe microscopy of electronic transport in carbon nanotubes *Phys. Rev. Lett.* **84** 6082–5
- [24] Bauer E, Munschau M, Swiech W and Teliens W 1989 Surface studies by low-energy electron-microscopy (LEEM) and conventional UV photoemission electron-microscopy (PEEM) *Ultramicroscopy* **31** 49–57
- [25] Ballarotto V W, Breban M, Siegrist K, Phaneuf R J and Williams E D 2002 Photoelectron emission microscopy of ultrathin oxide covered devices *J. Vac. Sci. Technol. B* **20** 2514–8
- [26] Gunther S, Kolmakov A, Kovac J and Kiskinova M 1998 Artifact formation in scanning photoelectron emission microscopy *Ultramicroscopy* **75** 35–51
- [27] Gilbert B, Andres R, Perfetti P, Margaritondo G, Rempfer G and De Stasio G 2000 Charging phenomena in PEEM imaging and spectroscopy *Ultramicroscopy* **83** 129–39
- [28] Karam R M and Casler R J 2004 A new 3D, direct-write, sub-micron microfabrication process that achieves true optical, mechatronic and packaging integration on glass-ceramic substrates *Photonics Cluster (UK newsletter) vol 7* <http://www.photonicscluster-uk.org/newsletter/winter04/accelonix.pdf>